THE JOURNAL OF BIOLOGICAL CHEMISTRY
Vol. 278, No. 7, Issue of February 14, pp. 4963–4971, 2003
Printed in U.S.A.

Enzymatic and Structural Analysis of Inhibitors Designed against *Mycobacterium tuberculosis* Thymidylate Kinase

NEW INSIGHTS INTO THE PHOSPHORYL TRANSFER MECHANISM*

Received for publication, September 19, 2002, and in revised form, November 25, 2002
Published, JBC Papers in Press, November 25, 2002, DOI 10.1074/jbc.M209630200

Ahmed Haouz‡, Veerle Vanheusden§, Hélène Munier-Lehmann¶, Mattheus Froeyen‖, Piet Herdewijn‖, Serge Van Calenbergh§, and Marc Delarue‡**

From the ‡Unité de Biochimie Structurale and ¶Laboratoire de Chimie Structurale des Macromolécules, URA 2185 du CNRS, Biologie Structurale et Agents Infectieux, Institut Pasteur, 25 rue du Dr Roux, 75015 Paris, France, the §Laboratory of Medicinal Chemistry, Faculty of Pharmaceutical Sciences, Ghent University, Harelbekestraat 72, B-9000 Ghent, Belgium, and the ‖Laboratory of Medicinal Chemistry, Rega Institute for Medical Research, Catholic University of Leuven, Minderbroedersstraat 10, B-3000 Leuven, Belgium

The chemical synthesis of new compounds designed as inhibitors of *Mycobacterium tuberculosis* TMP kinase (TMPK) is reported. The synthesis concerns TMP analogues modified at the 5-position of the thymine ring as well as a novel compound with a six-membered sugar ring. The binding properties of the analogues are compared with the known inhibitor azido-TMP, which is postulated here to work by excluding the TMP-bound Mg^{2+} ion. The crystallographic structure of the complex of one of the compounds, 5-CH_2OH-dUMP, with TMPK has been determined at 2.0 Å. It reveals a major conformation for the hydroxyl group in contact with a water molecule and a minor conformation pointing toward Ser^{99}. Looking for a role for Ser^{99}, we have identified an unusual catalytic triad, or a proton wire, made of strictly conserved residues (including Glu^6, Ser^{99}, Arg^{95}, and Asp^9) that probably serves to protonate the transferred PO_3 group. The crystallographic structure of the commercially available bisubstrate analogue P^1-(adenosine-5′)-P^5-(thymidine-5′)-pentaphosphate bound to TMPK is also reported at 2.45 Å and reveals an alternative binding pocket for the adenine moiety of the molecule compared with what is observed either in the *Escherichia coli* or in the yeast enzyme structures. This alternative binding pocket opens a way for the design of a new family of specific inhibitors.

The incidence of tuberculosis has been increasing during the last 20 years; it is now the first cause of mortality among infectious diseases in the world (1). The combination of four active drugs (rifampicin, isoniazid, pyrazinamide, and ethambutol or streptomycin) is currently used in *Mycobacterium tuberculosis* treatment, but this has led to the appearance of resistant bacterial strains (2). These resistant strains are alarming for two reasons. First, as there are only a few effective drugs available, infection with drug-resistant strains could give rise to a potentially untreatable form of the disease. Second, although only 5% of immunocompetent people infected with *M. tuberculosis* succumb to the disease, it is nevertheless highly contagious (3). Therefore, a large effort is necessary to identify potential new targets and inhibitors.

An attractive potential target is thymidylate kinase (EC 2.7.4.9, ATP:TMP phosphotransferase, TMPK),[1] an essential enzyme that catalyzes an obligatory step in the synthesis of TTP either from thymidine via thymidine kinase (salvage pathway) or from dUMP via thymidylate synthase in all living cells (4). This enzyme phosphorylates TMP into TDP using ATP as the preferred phosphoryl donor.

In the case of the herpes simplex virus (HSV), the most successful antiviral drug (acyclovir) available on the market is directed against thymidine kinase. Acyclovir is phosphorylated by several viral or host kinases into acyclovir triphosphate, which terminates DNA synthesis when incorporated into the viral DNA (5, 6). The comparative x-ray structures of different enzyme-ligand complexes of HSV type 1 thymidine kinase (7–10) revealed a number of interesting structural features and paved the way for rational structure-based drug design of antiviral compounds (11, 12). A similar approach might lead to potent antituberculosis agents.

TMPK from *M. tuberculosis* is a homodimer with 214 amino acids per monomer (13). The x-ray three-dimensional structure has been recently solved at 1.95-Å resolution (14, 15) as a complex with TMP, thereby making it possible to initiate structure-based drug design studies. The global folding of the protein is similar to that of the others TMPKs and NMP kinases despite the low similarity of their amino acid sequences. The TMP kinase backbone is characterized by nine solvent-exposed α-helices surrounding a central β-sheet made of five β-strands, typical of the so-called Rossmann-fold (16–20). However, the dimerization mode of the *M. tuberculosis* enzyme differs from that reported in the yeast, human, and *Escherichia coli* enzymes (15).

The active site of *M. tuberculosis* TMP kinase complexed with TMP differs from the other known TMPKs in the following ways (15). It is in a fully closed conformation with the ATP binding site being already preformed and the LID region well ordered into a α-helical conformation even though the second substrate ATP (or non-hydrolyzable ATP) is absent from the

* This work was supported by Grant BIO-CT98-0354 from the European Economic Community (to both M. D. and P. H.). The costs of publication of this article were defrayed in part by the payment of page charges. This article must therefore be hereby marked "*advertisement*" in accordance with 18 U.S.C. Section 1734 solely to indicate this fact.

The atomic coordinates and structure factors (code 1MRS and 1MRN) have been deposited in the Protein Data Bank, Research Collaboratory for Structural Bioinformatics, Rutgers University, New Brunswick, NJ (http://www.rcsb.org/).

** To whom correspondence should be addressed. Tel.: 33-1-45-68-86-01; Fax: 33-1-45-68-86-04; E-mail: marc.delarue@pasteur.fr.

[1] The abbreviations used are: TMPK, TMP kinase; Ap_5T, P^1-(adenosine-5′)-P^5-(thymidine-5′)-pentaphosphate; HSV, herpes simplex virus; W, water; HPLC, high pressure liquid chromatography; AZTMP, azido-TMP; Mtub, *M. tuberculosis*; iPrOH, isopropanol.

structure. In the TMP binding site, the protein-TMP interaction shows three specific features when compared with yeast, human, or *E. coli* enzyme structures. The first feature involves both a magnesium ion and Tyr^{39}; they interact with two opposite non-bridging oxygens of the phosphate moiety of TMP. The second feature involves Asn^{100} in contact with atom N-3 of the base moiety (15). The third feature, perhaps more amenable to the design of new inhibitors, is the interaction of the 3′-OH atom of TMP with both the side chain of Asp^{9} and a water molecule, W9, which is a ligand of the Mg^{2+} ion. In addition, there is a high concentration of positively charged side chains both from the LID region and from the P-loop with arginine residues 14, 95, 149, and 160 as well as Lys^{13} (15). Examination of the structure therefore suggested the following targets for species-specific inhibitors. In target 1, the 3′-OH and 2′-OH groups of the ribose ring could be systematically replaced with different chemical groups; this has been recently reported (21). In target 2, the 5-position of the thymine ring is another possibility that has also been considered in the past for HSV thymidine kinase inhibitors (*e.g.* Refs. 11 and 12). Preliminary results of compounds modified at this position have already been reported (13). Here we report results on other compounds with the aim of adding an extra hydrogen bond with water molecule W12 detected in the three-dimensional structure. W12 is located close to Pro^{37} (which is in a cis conformation) and forms hydrogen bonds with residues building up the thymidine binding cavity, such as Phe^{70}, Asp^{73}, and Arg^{74}. In target 3, the 2-position of the thymine ring could also be explored, and preliminary but encouraging results have been reported for one compound modified at this position (13). The aim here is to replace the inserted (space-filling) water molecules W2 and W3 that, if removed, give rise to a well defined cavity that can be readily materialized with computer programs such as VOIDOO (22).

In this study we have synthesized five TMP analogues (**1–5**, Fig. 1), modified at the thymine moiety and focused on target 2. In addition, one member of a new class of nucleotide analogues has been tested (23, 24), namely a 1,5-anhydrohexitol analogue (**6**) of TMP, where the 3′-OH and/or the 5′-*O*-phosphate positions are expected to depend on the sugar conformation. The inhibitory effect of these TMP analogues has been measured *in vitro* by a novel direct specific enzymatic activity test using HPLC and compared with the reference compound AZTMP, which is a good inhibitor (13).

All compounds have been subjected to co-crystallization experiments as well as soaking experiments for exchange with TMP in TMP-TMPK crystals (*M. tuberculosis* TMPK does not crystallize in the absence of TMP). We solved the structure of one promising enzyme-inhibitor complex by x-ray diffraction and have determined the rearrangement of side chains in the active site and the concomitant modification of the water molecule network around the thymine moiety of the TMP substrate. In addition, we have co-crystallized and solved the structure of the complex between TMP kinase and the bisubstrate analogue Ap_5T. Altogether, considerable new insight into the possible mechanism of phosphoryl transfer has been gained as described at the end of the "Discussion."

EXPERIMENTAL PROCEDURES

Protein and Reagents

The *M. tuberculosis* (Mtub) TMP kinase was overexpressed in *E. coli* and purified as described previously (13). The protein was stored at −20 °C in aliquots of 100 μl at 4 mg/ml in a buffer containing 20 mM Tris-HCl, pH 7.5, 0.5 mM dithiothreitol, and 1 mM EDTA, conditions at which it is stable over several months. Ap_5T was purchased from Jena Bioscience (Germany). All other reagents used were purchased from Sigma, including the reference inhibitor AZTMP. All solutions were made with pyrolyzed water.

Inhibitor Synthesis

Several methods have already been reported for the synthesis of 5-hydroxymethyl-2′-deoxyuridine. We found that hydroxymethylation of 2′-deoxyuridine with formaldehyde under acidic (25) or basic (26) catalysis gave only low yields. Therefore, we decided to couple 5-benzyloxymethyluracil with an appropriate sugar. In Ref. 27, the base is coupled with 1,2,3,5-tetracetylribose. Since this method requires subsequent 2′-deoxygenation, we chose to glycosylate the silylated base with 2-deoxy-3,5-*O*-di-(toluoyl)-α-D-*erythro*-pentafuranosylchloride (28). Unfortunately racemization of the sugar prior to coupling led to a hardly separable mixture of the α- and β-anomers of the protected nucleoside. After alkaline removal of the acyl groups, however, the anomeric mixture could be separated via column chromatography to give the α- and β-anomers **10** and **11** as white foams. Both isomers were then phosphorylated. We noticed that the 5-*O*-benzyl group got partly removed during this step. Thus phosphorylation of the β-nucleoside gave three compounds: 2′-deoxy-5-hydroxymethyl-5′-*O*-phosphoryluridine (**1**), its benzyl-protected analogue (**2**), and 2′-deoxy-5-hydroxymethyluridine (**12**). Phosphorylation of the α-nucleoside gave the corresponding benzylated and non-benzylated nucleotides **13** and **3** (Scheme 1).

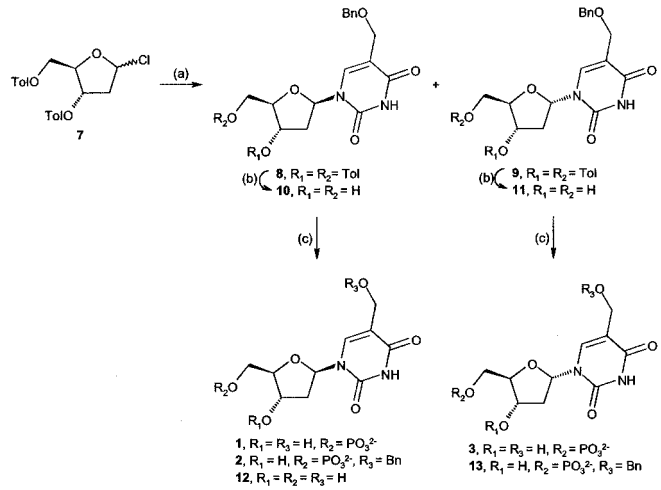

SCHEME 1. **Reagents and conditions.** *a*, 5-bensyloxymethyl-2,4-bis[(trimethylsilyl)oxy]pyrimidine, CH_3CN; *b*, NH_3, MeOH; c, $POCl_3$, $(MeO)_3PO$.

2′-Deoxy-5-(2-furyl)uridine (**15**) and 2′-deoxy-5-(thien-2-yl)uridine (**16**) were synthesized according to a published procedure from unprotected 2′-deoxy-5-iodouridine (**14**) (29). Phosphorylation of these two nucleosides yielded the two desired 5-heteroaryl-substituted nucleotides **4** and **5** (Scheme 2).

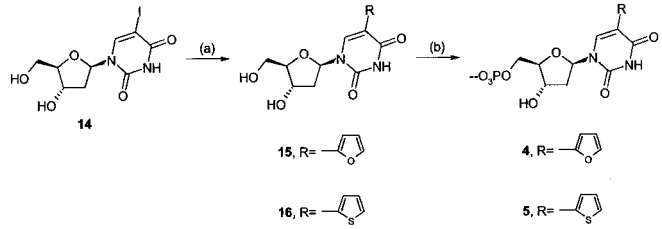

SCHEME 2. **Reagents and conditions.** *a*, 2-(tributylstannyl)furan, $(Ph_3P)_2Pd(II)Cl_2$, dioxane or 2-(tributylstannyl)thiophene, $Pd(OAc)_2$, Ph_3P, Et_3N, dioxane; *b*, POCl3, $(MeO)_3PO$.

Synthesis: General—NMR spectra were obtained with a Varian Mercury 300 or 500 spectrometer using the solvent signal of Me_2SO-d_6 as a secondary reference. All signals assigned to amino and hydroxyl groups were exchangeable with D_2O. Mass spectra and exact mass measurements were performed on a quadrupole/orthogonal-acceleration time-of-flight tandem mass spectrometer (qTof 2, Micromass, Manchester, UK) equipped with a standard electrospray ionization interface. Samples were infused in a 2-propanol:water (1:1) mixture at 3 μl/min. If necessary, nucleoside 5-*O*-monophosphates were ultimately purified using a Gilson HPLC system with a Gilson 322 pump, a UV/VIS-156 detector on a C18 column (10 μM, Altech, Altima, 250 × 22 mm). Precoated Merck silica gel F_{254} plates were used for TLC, and spots

were examined with UV light at 254 nm and sulfuric acid-anisaldehyde spray or phosphomolybdic acid (0.5% in EtOH) solution. Column chromatography was performed on Uetikon 560 silica (0.2–0.06 mm) and Amersham Biosciences DEAE-Sephadex™ A-25.

The ^1H (and ^{31}P, if appropriate) NMR spectra allowed the characterization of all purified intermediates in the synthesis and final products and are available from the authors upon request. In all instances, mass spectra were found to give the calculated mass within experimental error.

*5-Benzyloxymethyl-1-[2-deoxy-3,5-O-di-(toluoyl)-β-D-erythro-pentafuranosyl]thymine (**8**) and 5-Benzyloxymethyl-1-[2-deoxy-3–5-O-di-(toluoyl)-α-D-erythro-pentafuranosyl]thymine (**9**)*—5-Benzyloxymethyluracil (680 mg, 2.93 mmol) was suspended in a mixture of hexamethyldisilazane (62 ml), trimethylsilyl chloride (0.5 ml, 3.94 mmol), and pyridine (5 ml). The mixture was refluxed overnight. The resulting solution was evaporated and co-evaporated with toluene. The obtained residue was suspended in anhydrous CH_3CN (3.5 ml), and 2-deoxy-3,5-*O*-di-(toluoyl)-α-D-*erythro*-pentofuranosyl chloride (1 g, 2.58 mmol) was added. The reaction mixture was stirred for 3 h at room temperature. CH_2Cl_2 (25 ml) was added, and the organic layer was washed with a 7% solution of $NaHCO_3$ (25 ml). The water layer was washed twice with CH_2Cl_2 (25 ml). The combined organic layers were dried over $MgSO_4$ and evaporated. The residue was purified by column chromatography (silica, CH_2Cl_2:MeOH 98:2) to give a mixture of α- and β-anomers (0.932 g, 62%). The anomers were partly separated by a combination of precipitation (ether:MeOH 13:8) and column chromatography (silica, CH_2Cl_2:MeOH 100:0 → 99:1 → 98:2). The two mixtures, enriched in either anomer, were used without further purification in the next step.

*1-(2-Deoxy-β-D-erythro-pentofuranosyl)-5-(benzyloxymethyl)thymine (**10**) and 1-(2-Deoxy-α-D-erythro-pentofuranosyl)-5-(benzyloxymethyl)thymine (**11**)*—A mixture of **8** and **9** (932 mg, 1.70 mmol) was dissolved in EtOH (60 ml), and 2 N NaOH (37 ml) was added. The mixture was stirred at room temperature for 15 min and evaporated. The obtained residue was dissolved in 5 ml of H_2O and neutralized with HCl. The precipitate was filtered, and the filtrate was evaporated and co-evaporated with EtOH. The obtained residue was purified by column chromatography (silica, CH_2Cl_2:MeOH 93:7) to give **10** (261 mg, 44%) and **11** (284 mg, 48%) as white foams.

*1-(2-Deoxy-5-O-phosphoryl-β-D-erythro-pentofuranosyl)-5-(hydroxymethyl)thymine (**1**), 1-(2-Deoxy-5-O-phosphoryl-β-D-erythro-pentofuranosyl)-5-(benzyloxymethyl)thymine (**2**), and 1-(2-Deoxy-β-D-erythro-pentofuranosyl)-5-(hydroxymethyl)thymine (**12**)*—A solution of **10** (261 mg, 0.75 mmol) in trimethyl phosphate (3.5 ml) was cooled to 0 °C, $POCl_3$ (0.22 ml, 2.4 mmol) was added dropwise, and the mixture was stirred for 4 h at 0 °C. The mixture was poured into crushed ice-water (20 ml), neutralized with concentrated NH_4OH, and evaporated to dryness. The residue was subjected to column chromatography (silica, iPrOH:NH_4OH:H_2O 77.5:15:2.5 → 60:30:5) yielding **12** (38.7 mg, 20%) as a white foam as well as an oily mixture of **1** and **2**. This mixture was further purified by HPLC (C18, CH_3CN:MeOH:0.05% HCOOH in H_2O 45:45:10, 3 ml/min), and the fractions containing the nucleotides were lyophilized yielding **2** (47 mg, 14%) and **1** (109 mg, 41%) as white powders.

*1-(2-Deoxy-5-O-phosphoryl-α-D-erythro-pentofuranosyl)-5-(hydroxymethyl)thymine (**3**) and 1-(2-Deoxy-5-O-phosphoryl-α-D-erythro-pentofuranosyl)-5-(benzyloxymethyl)thymine (**13**)*—A solution of **11** (248 mg, 0.71 mmol) in trimethyl phosphate (3.5 ml) was cooled to 0 °C, $POCl_3$ (0.21 ml, 2.3 mmol) was added dropwise, and the mixture was stirred for 4 h at 0 °C. The mixture was poured into crushed ice-water (20 ml), neutralized with NH_4OH, and evaporated to dryness. **3** and **13** were separated by column chromatography (silica, iPrOH:NH_4OH:H_2O 77.5:15:2.5 → 60:30:5). Further purification was accomplished by HPLC (C18, CH_3CN:MeOH:0.05% HCOOH in H_2O 45:45:10, 3 ml/min). The fractions containing the principal nucleotides were lyophilized yielding **3** (106 mg, 42%) and **13** (47 mg, 15%) as white powders.

*2′-Deoxy-5-(2-furyl)-5′-O-phosphoryluridine (**4**)*—A solution of **15** (382 mg, 1.22 mmol) in trimethyl phosphate (5.8 ml) was cooled to 0 °C. $POCl_3$ (0.4 ml, 4.29 mmol) was added dropwise, and the mixture was stirred for 4 h at 0 °C. It was poured into crushed ice-water (40 ml), neutralized with NH_4OH, and evaporated to dryness. The resulting residue was purified by column chromatography (silica, iPrOH:NH_4OH:H_2O 77.5:15:2.5 → 60:30:5). The obtained white powder was further purified on DEAE-Sephadex A-25 (triethylammoniumbicarbonate 0 → 0.5 M) yielding the triethylammonium salt of **4**. This was converted to its corresponding sodium salt (NaI, acetone) (248 mg, 51%) as a white powder.

*2′-Deoxy-5-(thien-2-yl)-5′-O-phosphoryluridine (**5**)*—A solution of **16** (320 mg, 1.03 mmol) in trimethyl phosphate (4.6 ml) was cooled to 0 °C, $POCl_3$ (0.31 ml, 3.3 mmol) was added dropwise, and the mixture was stirred for 4 h at 0 °C. The mixture was poured into crushed ice-water (20 ml), neutralized with 28% ammonia, and evaporated to dryness. The resulting residue was purified by column chromatography (silica, iPrOH:NH_4OH:H_2O 77.5:15:2.5 → 60:30:5). The obtained white powder was further purified on DEAE-Sephadex A-25 (triethylammonium bicarbonate 0 → 0.5 M) yielding the triethylammonium salt of **5**. This was converted to its corresponding sodium salt (NaI, acetone) (240 mg, 57%) as a white powder.

Enzymatic Assay

The TMP kinase activity was measured by HPLC separation of nucleotide substrates and products as described below. The major reason for using this test instead of the more rapid coupled spectrophotometric assay (30) is that some inhibitors absorb light at 340 nm (**4** and **5**), thereby rendering difficult the evaluation of NADH concentration in the coupled reaction. Also, coupled enzymatic tests might be error-prone in the determination of the true value of K_i and K_m of inhibitors and substrate, respectively, through the recycling of some substrate or product during the reaction coupling (31). The reaction is carried out in a 1-ml final volume of a solution of 50 mM Tris-HCl, pH 7.5, 20 mM magnesium acetate, 100 mM KCl, 1 mM EDTA, 0.5 mM dithiothreitol using different initial concentrations of ATP and TMP in the presence or absence of various inhibitors. To follow the enzymatic kinetics an aliquot of 100 μl is taken at different times after enzyme addition, and the reaction is quenched by adding 900 μl of 100 mM sodium phosphate, pH 7. The concentration of each nucleotide at different times during the reaction is measured at 260 nm by HPLC (isocratic mode) using a Sephasil™ C18, 5-μm SC 2.1/10 (Amersham Biosciences) column. The buffer used for elution is 50 mM sodium phosphate, pH 6.5, 2.5% (v/v) ethanol, 40 mM tetrabutylammonium bromide with a flow rate of 250 μl/min. All the reaction velocities are calculated by monitoring the production of TDP expressed in terms of optical absorbance per minute at 260 nm. It was checked that all four sources of information (appearance of TDP or ADP, disappearance of ATP or TMP) can be used and lead to the same results (see also Ref. 11).

Crystallization and Diffraction Data Collection

Co-crystals of *M. tuberculosis* TMPK in complex with compound **1** (see Fig. 1) were obtained as described for crystals with the TMP substrate (14). Briefly a 6-μl drop of a 1:1 mixture of the protein solution (3.5 mg/ml) incubated overnight with 5 mM analogue **1** and the reservoir solution was equilibrated with 34% (w/v) ammonium sulfate solution, 100 mM HEPES, pH 6.0, containing 2% (w/v) polyethylene glycol 2000, 20 mM magnesium acetate, and 0.5 mM β-mercaptoethanol. Crystals grew in 1–3 weeks to bipyramids of 400 × 200 × 200 μm^3. X-ray data were collected from cryo-cooled crystals using 25% (w/v) glycerol as cryoprotectant.

Soaking experiments were performed by first transferring TMP-TMPK co-crystals to a stabilizing solution containing 70% ammonium sulfate and 1 mM TMP and then to a fresh solution containing 70% ammonium sulfate and 10 mM inhibitor (but no TMP). This last solution was replaced three times, each soaking time lasting 24 h.

Diffraction data were processed using the DENZO/SCALEPACK (32) package. The CCP4 package (33) was used to calculate structure factors from the observed intensities (TRUNCATE). Reflections in the resolution ranges 2.28–2.22 and 2.70–2.64 Å had to be suppressed due to the presence of ice rings during data collection for the **1**-TMPK complex.

Model Building and Refinement

Refinement was performed up to 2.0-Å resolution with CNS (34). Standards protocols, including maximum likelihood target, bulk solvent correction, and isotropic B-factors, were used (34, 35). The model was inspected manually with SIGMAA-weighted $2F_o - F_c$ and $F_o - F_c$ maps (36), and progress in the model refinement was evaluated by the decrease in the free *R*-factor. Manual rebuilding in the electron density maps was done with O (37). Stereochemistry of the final model was assessed using PROCHECK (38). Coordinates of the **1**-$TMPK_{Mtub}$ binary complex have been deposited in the Research Collaboratory for Structural Bioinformatics (RSCB) Protein Data Bank (accession code 1MRS). Similar structural details apply to the Ap_5T-TMPK complex where all the dictionaries necessary for O and CNS come from the data base of G. Kleywegt.[2] The coordinates have

[2] HIC-Up, available at alpha2.bmc.uu.se/hicup/t5a.

TABLE I
Apparent inhibition constant (K_i^{app}) of different synthesized inhibitors

Analogue no. or name	5-Position of the pyrimidine ring	1′ (sugar)	5′ (sugar)	3′ (sugar)	K_i^{app}
					μM
1[a]	CH_2OH	β	Phosphate	OH	110
2[a]	CH_2-O-CH_2-phenyl	β	Phosphate	OH	280
3[a]	CH_2OH	α	Phosphate	OH	450
4[a]	Furan-2-yl	β	Phosphate	OH	140
5[a]	Thien-2-yl	β	Phosphate	OH	270
BVDU[b]	CH═CHBr	β	OH	OH	900
Thymidine	CH_3	β	OH	OH	280
dUMP (8)	Hydrogen	β	Phosphate	OH	Substrate
5-F-dUMP (8)	Fluorine	β	Phosphate	OH	Substrate
5-Br-dUMP (8)	Bromine	β	Phosphate	OH	Substrate
5-I-dUMP (8)	Iodine	β	Phosphate	OH	Substrate
6[a]	CH_3	Hexose	Phosphate	OH	150
AZTMP	CH_3	β	Phosphate	N_3	50
Ap_5T	CH_3	β	p_5A[c]	OH	30

[a] See Fig. 1 for the structures of compounds **1–6.**
[b] BVDU, (*E*)-5-(2-bromovinyl)-2′-deoxyuridine.
[c] p_5A, adenosine 5′-pentaphosphate.

been deposited in the RSCB Protein Data Bank (accession code 1MRN).

RESULTS

Enzymatic Test: Calibration with the Natural Substrates—In all experiments, the enzyme concentration was set to a value at least 200 times lower than the substrates concentrations, *i.e.* typically 5×10^{-8} M. The reaction catalyzed by TMP kinase was found to follow the Michaelis model (39). The initial velocity of the reaction at different fixed (saturating) concentrations of ATP and different concentrations of TMP allows for the determination of the apparent K_m for TMP and for ATP. With this protocol we find an apparent K_m = 40 μM TMP. For ATP, we measured K_m = 100 μM. Both values compare well with the values obtained with the coupled assay (13). The K_m of 40 μM for TMP has been measured at the fixed concentration of ATP of 0.5 mM and shows some dependence upon ATP concentration. The K_m value of TMP extrapolated at zero ATP concentration is 4–5 μM in agreement with results reported earlier (13).

The role of ATP as the phosphoryl donor has been explored in Ref. 13 where other NTPs were tried and found to be less efficient than ATP. Similar results were obtained using the direct assay method described here (data not shown).

Inhibition of TMP Kinase Activity with Synthetic Compounds—Measuring the initial velocity of the reaction at a fixed saturating concentration of ATP and different concentrations of TMP, both in the absence and presence of inhibitors, allows the testing of the nature of the inhibition (39, 40). In our case, the reciprocal plot confirms that all inhibitors are competitive with TMP because the least-squares-fitted best lines in the absence and presence of the inhibitor cross exactly on the *y* axis. In the classical competitive inhibition model (with the Lineweaver-Burk representation), we can use Equation 1 (39).

$$K'_m = K_m\left(1 + \frac{[I]}{K_i}\right) \qquad \text{(Eq. 1)}$$

where K'_m and K_m are the apparent Michaelis constants determined in the presence and absence of inhibitor, respectively. Knowing the concentration of inhibitor [*I*], it is possible to calculate K_i, which is shown in Table I.

For AZTMP, the dependence of the K_i value upon ATP concentration was found to be significant in accordance with Ref. 13. However, for all the inhibitors reported here, we report only the apparent K_i value at the fixed concentration of ATP of 1.0 mM. AZTMP will serve as a reference compound here since our aim is to do better than this compound.

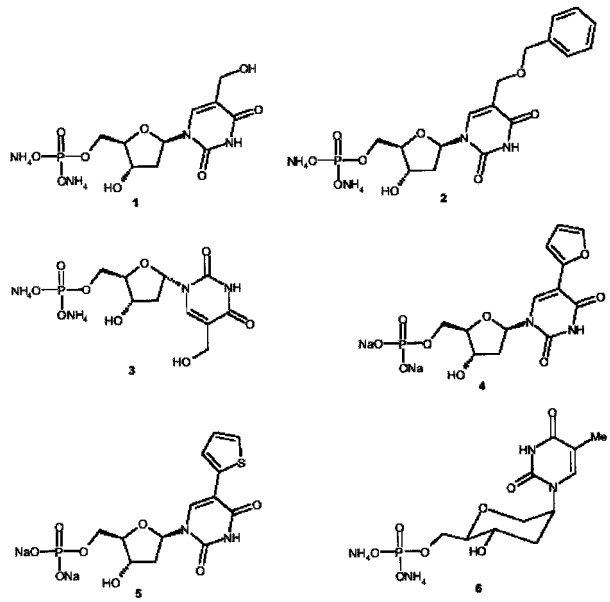

FIG. 1. **Chemical structure of synthesized TMP analogues.**

Exploring the 5-Position of the Thymine Ring—Systematic substitution of the methyl group in the 5-position of the base into halogen atoms was explored in Ref. 8. Bromine, which has the same size as CH_3, was found previously to be very similar to TMP in terms of both K_i and V_{max} (13). The difference in the kinetic parameters of these compounds reflects essentially a size effect with the halogen atoms serving as cavity-filling atoms. In this work other compounds substituted at the 5-position of the base moiety of TMP have been synthesized and will be described here.

Nucleotide analogue **1** was designed in an effort to induce an additional contact between the 5-CH_2OH group and the side chain of Arg^{74}. The value of the K_i constant indicates a moderately active inhibitor as compared with AZTMP (Table I).

Other TMP analogues were synthesized in which the volume of the substituent at this position was further increased while maintaining one polar atom, namely a thiophene and a furane derivative. The resulting compounds (**4** and **5**) were less active than the 5-CH_2OH-dUMP, indicating that the volume of this cavity cannot be stretched too much. Another compound (**2**) aiming toward a stacking interaction with the Phe^{36} residue resulted in a less active compound (Table I). The unnatural

TABLE II
*Data collection statistics of the TMPK-**1** and TMPK-Ap$_5$T complexes*

	TMPK-**1** cocrystals	TMPK-Ap$_5$T cocrystals
X-ray source	ESRF,[a] ID14–3	Rotating anode (laboratory)
Wavelength (Å)	0.940	1.5418
Detector	MARCCD	MAR-IP
Space group	P6$_5$22	P6$_5$22
$a = b$, c (Å)	76.34, 134.42	75.48, 133.35
Resolution (Å)	25.0–2.00 (2.07–2.00)	30.0–2.45 (2.54–2.45)
Total of unique reflections	14,739 (1,575)	8,407 (768)
Multiplicity	6.0 (5.9)	3.3 (3.0)
Completeness (%)	89.5 (98.6)	95.1 (90.1)
R_{merge}[b]	0.082 (0.271)	0.066 (0.366)
$I/\sigma(I)$	27.8 (18.8)	10.2 (9.2)

[a] ESRF, European Synchrotron Radiation Facility.
[b] $R_{merge} = \Sigma_h\Sigma_i|I_{hi} - \langle I_h\rangle|/\Sigma_h\Sigma_i I_{hi}$, where I_{hi} is the ith observation of the reflection h, while $\langle I_h\rangle$ is the mean intensity of reflection h.

TABLE III
*Refinement statistics of the TMPK-**1** and the TMPK-Ap$_5$T complexes*

	1-TMPK	Ap$_5$T-TMPK
Resolution range (Å)	25.0–2.00	30.0–2.45
Cut-off I/σ (I)	1.0	0.1
No. of reflections used for refinement	12,400	7,769
No. of reflections used for R_{free} calculation	641	379
No. of non-hydrogen atoms		
Protein	1,543	1,543
Inhibitor	22	53
SO_4^- (two molecules)	10	10
Mg^{2+}	1	1
Water	77	58
Refinement statistics		
R_{factor}[a] (%)	22.8	23.6
R_{free}[b] (%)	26.5	28.4
r.m.s.[c] deviations from ideality		
Bond lengths (Å)	0.0068	0.0079
Bond angles (°)	1.19	1.21
Dihedral angles (°)	20.67	20.1
Average temperature factors		
Main chain	35.35	38.2
Side chain atoms	38.2	39.2
Inhibitor	31.2	40.4
SO_4^- molecule 1 (molecule 2)	30.1 (34.4)	30.1 (36.2)
Mg^{2+}	46.96	34.5
Water	43.7	42.6
Scaling parameters (F_{calc} to F_{obs}: k (e/Å^3) and B (Å^2))	0.333 (50.5)	0.359 (42.56)
Ramanchandran plot		
Residues in most favoured regions (%)	96.1	91.1
Residues in additional allowed regions (%)	3.4	8.4
Residue in disallowed regions (%)	0.5 (Arg^{95})	0.5 (Arg^{95})
Overall G-factor[d]	0.36	0.31

[a] $R_{factor} = \Sigma||F_o| - |F_c||/|F_o|$.
[b] R_{free} is calculated with 5% of randomly selected reflections.
[c] r.m.s., root mean square.
[d] G-factor is an overall measure of the structure quality calculated with PROCHECK (38).

α-isomer of **1** was also synthesized (**3**, see Fig. 1) and assayed but proved less active than **1** (see Table I).

Another possibility would be to increase the length of the linker from the C-5 position up to a polar atom to replace directly the W12 water molecule, which is located at 3.95 Å from the C-5 atom of TMP behind the pyrrolidine ring of Pro^{37}. Pro^{37} has a cis-peptide bond conformation that is maintained through a hydrogen bond between its carbonyl atom and a water molecule, W26, which is also in contact with one of the oxygens of the phosphate group of TMP. Therefore, the exact position of Pro^{37} is expected to be important for catalysis. This cis-peptide bond is also present in the three other known structures of TMP kinases (16–20). The deoxyribose analogue of dU with a substituent of exactly the size to reach out for the water molecule W12 (-CH=CH-Br) has been studied and compared with dT. This compound, (*E*)-5-(2-bromovinyl)-2′-deoxyuridine, has already proved efficient for inhibition of HSV type 1 thymidine kinase (12). It was predicted that the electronegative bromine atom would play the role of W12. However, this compound proved relatively inefficient for *M. tuberculosis* TMPK (Table I).

Inhibition by Ap$_5$T—The bisubstrate analogue Ap$_5$T has been found to be more efficient than AZTMP with an inhibition constant K_i = 30 μM, making it one of the most powerful inhibitors of *M. tuberculosis* TMP kinase known to date. This compares well with similar inhibitors designed against other NMP kinases (18, 41). The inhibition mechanism inferred from the reciprocal plot analysis is compatible with the one described for adenylate kinase where it is a competitive inhibitor for the forward reaction and a mixed noncompetitive inhibitor for the backward reaction (42). To understand the chemical nature of the interaction of this inhibitor with its target and to further increase the efficiency of this compound, the structure determination of its complex with its TMPK was undertaken (see below).

Inhibition by the 1,5-Anhydrohexitol Analogue of TMP—Modification of the sugar moiety of TMP into a 1,5-anhydrohexitol was performed (**6**). This analogue is actually a member

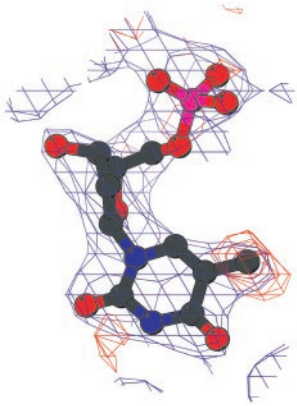

FIG. 2. **Electron density difference map around the analogue 1 (drawn with Bobscript (49)).** The $F_o - F_c$ SIGMAA-weighted map is contoured at 3.0 σ (*red*), while the $2F_o - F_c$ is contoured at 1.0 σ (*blue*).

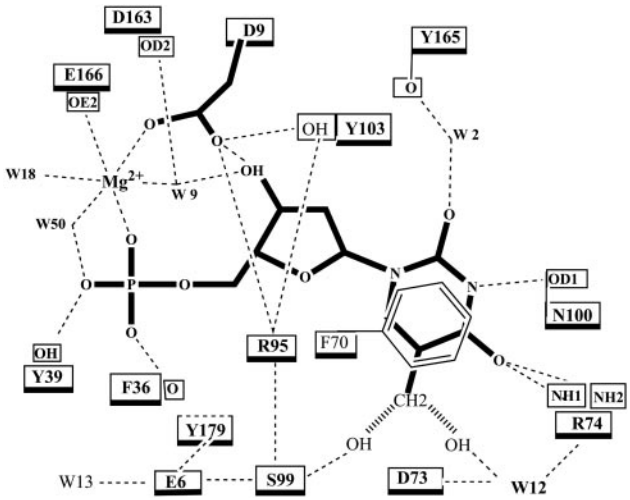

FIG. 3. **Network of interactions of the analogue 1 in the active site of TMP kinase (drawn with Chemdraw).**

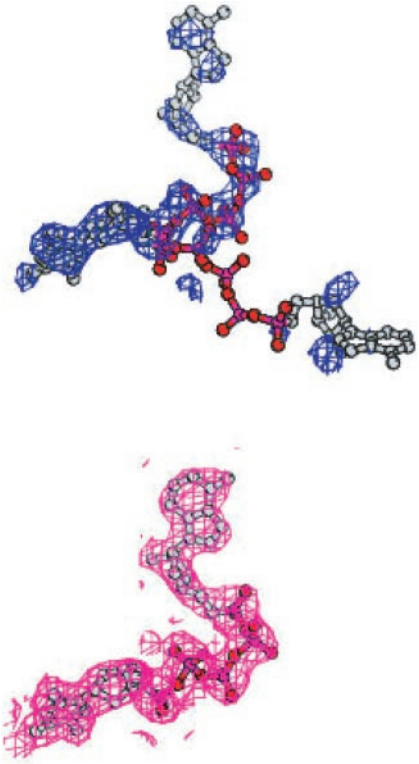

FIG. 4. **Electron density difference map around the Ap_5T compound (drawn with Bobscript (49)).** *Top*, the $F_o - F_c$ SIGMAA-weighted map with phases calculated with a model deprived of the inhibitor is contoured at 2.5 σ (*blue*). Both the refined model and the expected binding mode deduced from the structure of the same molecule in the *E. coli* TMPK complex are shown for comparison (ball and stick representation). *Bottom*, SIGMAA-weighted $2F_o - F_c$ map contoured at 1.0 σ (*magenta*).

of a novel series of inhibitors already tested against HSV type 1 thymidine kinase (24). The 5′-*O*-monophosphate was tested against *M. tuberculosis* TMPK but proved to be a moderately potent competitive inhibitor, again using AZTMP as a reference (see Table I).

Structure Determination of Bound Drugs in the TMP Binding Site of TMPK—To better understand the molecular origin of the differences in the K_i inhibition constants of all these compounds, we tried either to co-crystallize them with TMPK or to exchange them with TMP by soaking TMPK-TMP crystals with an excess of inhibitor.

No exchange of TMP by any of the analogues studied here was observed even after extensive soaking experiments on TMPK-TMP crystals in contrast with the control experiment with I-dUMP, which worked well as already reported in Ref. 15. However, one should bear in mind that I-dUMP is a substrate, whereas none of the compounds tried here are substrates.

No co-crystals were obtained except with compound **1**, whose structure was determined at 2.0-Å resolution (see Tables II and III for data collection and refinement statistics, respectively). The Fourier difference map clearly shows density for the OH group of CH_2OH (Fig. 2). The hydroxyl group makes an extra hydrogen bond with W12, which is also held in place by the side chain of Asp^{73} and the essential Arg^{74}. After inspection of the residual SIGMAA-weighted $F_o - F_c$ map, we found density at the 2.5 σ level for a possible alternative conformation of the hydroxyl group that reaches out for the side chain of the strictly conserved Ser^{99} (for which no definite role has yet been proposed). No attempt has been made to refine this alternative conformation since the limited resolution of our data makes it difficult to estimate their relative occupancies. Ser^{99} is part of a hydrogen bond network involving both Glu^6 (strictly conserved) and Tyr^{179} and helps to position correctly Arg^{95} (Fig. 3), which is strictly conserved among all known TMPKs except for the one from African swine fever virus where it is a histidine (15). Arg^{95} is the only residue of the whole protein whose main chain dihedral angles lie outside the "allowed" regions in a Ramachandran plot (Table III), an observation that holds true in the other structures of TMPKs known, so it must have an important functional role. The guanidinium group of Arg^{95} is located 3.2 Å away from the carboxylate group of Asp^9. Although the conformation of the side chain Arg^{95} is well conserved in the different TMPK structures, it has been shown that it can exist in another conformation in the complex with the products TDP and ADP, pointing toward the carbonyl of residue 36 just before the cis-peptide bond of Pro^{37} (17).

Structure Determination of Bound Ap_5T—The crystal structure of the complex of *M. tuberculosis* TMP kinase with Ap_5T has been determined at 2.45-Å resolution (see Tables II and III for data collection and refinement statistics, respectively). The structure reveals an unexpected binding mode for the adenine moiety of this compound. While the thymidine moiety of the bisubstrate analogue indeed occupies the binding pocket of the TMP substrate, the rest of the molecule departs from its expected position after the 5′-*O*-phosphate of the TMP moiety (Fig. 4). This is inferred from the superimposed crystal structures of both the *E. coli* and *Homo sapiens* enzymes complexed with the same bisubstrate analogue (18, 19). The phosphate backbone of the bound Ap_5T is making an angle of almost 90°

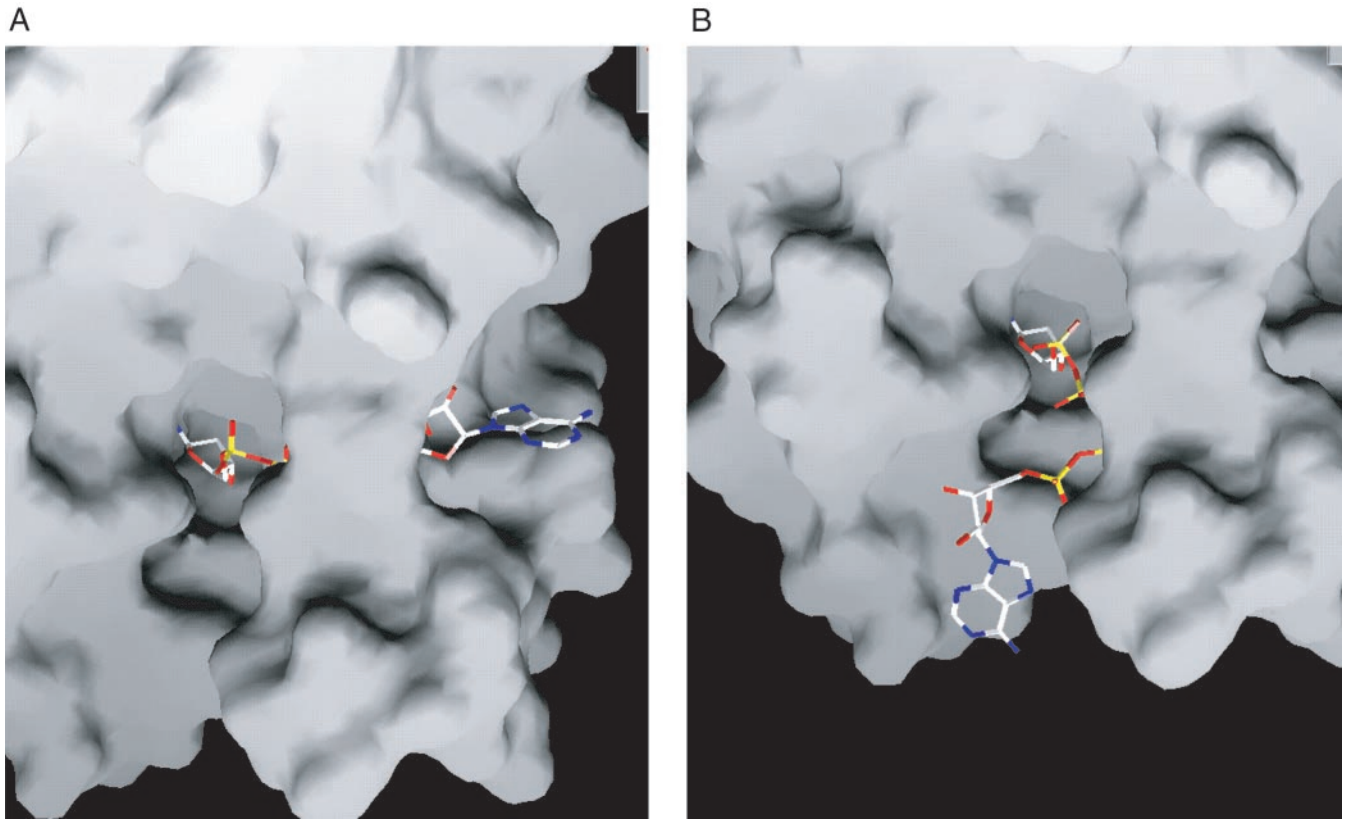

FIG. 5. **Comparison of the observed binding mode of Ap_5T both in the crystal state (*A*) and in the binding mode (*B*) expected from the structure of the same compound with the *E. coli* enzyme (19).** Surface representation was drawn using Grasp (50). The thymidine moiety of the molecule is hidden in its binding pocket.

with the superposed same molecule from *E. coli* at the α-phosphate. The surprise comes from the fact that the ADP moiety of the Ap_5T molecule snugly fits into a cavity on the surface of TMP kinase that appears to be specific to the *M. tuberculosis* enzyme (Fig. 5). This cavity involves packing interactions against helix α2 (residues 42–53) on one side and the region 152–162 on the other side. His^{53} is nicely stacked on the adenine ring.

DISCUSSION

One of the most striking findings of this study is that none of the 5-substituted dUMP analogues investigated here behave as a substrate for *M. tuberculosis* TMPK, contrary to what had been observed for halogen-substituted compounds at the same position (13, 15). Our current interpretation is that any modification that significantly perturbs the volume of the substituent at this position will change the orientation of the sugar moiety of the TMP molecule as well as that of the α-phosphate. Indeed, recent results obtained on a series of compounds modified at the 3′- and 2′-positions of the sugar (21) indicated an extreme sensitivity of the reaction to the exact positioning of at least the 3′-OH group of the sugar moiety, which is in a C2′-*endo* conformation in the active site. This is also illustrated in the present study with compound **6**, which behaves as an inhibitor probably because of its inability to place correctly both the 5′-*O*-phosphate and the 3′-OH groups in a favorable arrangement for catalysis.

Similarly, AZTMP is an inhibitor of the *M. tuberculosis* enzyme contrary to what is observed in TMPKs of other species (13) where it is either a weak substrate (in *H. sapiens*) or a good substrate (*E. coli*). This may be related to a unique feature of this enzyme revealed by its three-dimensional structure, namely the presence of a Mg^{2+} ion in the vicinity of Asp^9 and the 3′-OH position. Inhibition by AZTMP in the *M. tuberculosis* TMPK is probably due to a steric and/or electrostatic effect of the azido group, which would prevent the binding of the Mg^{2+} ion.

No Mg^{2+} ion has been observed in this position in any of the three other structures of TMPK reported so far (*E. coli*, yeast, and human enzymes) in various complexes (16–20). This is especially intriguing since most of the side chain ligands for the divalent cation observed in the *M. tuberculosis* are conserved in the three other known TMPK structures. A possible explanation for this phenomenon may be the peculiar coordination of the 5′-*O*-phosphate of TMP, which involves not only the Mg^{2+} ion but also Tyr^{39}, a specific feature of the *M. tuberculosis* sequence. Normally, at this Tyr^{39} position, an arginine or a lysine residue, as seen in the human, yeast, and *E. coli* enzyme structures and in the multialignment, is expected to neutralize the TMP phosphate negative charge. Since Tyr^{39} cannot play this role, it is tempting to postulate that this role is fulfilled by the Mg^{2+} cation in both *M. tuberculosis* and *Mycobacterium leprae* enzymes, but then the positive charge is located on the opposite side of the phosphate compared with the other known TMPKs, *i.e.* close to the essential Asp^9. Mg^{2+} may also contribute to deprotonate both the Asp^9 residue and the phosphate of TMP. We note that one of the water molecule ligands of the octahedral environment of the Mg^{2+} ion is likely to be replaced by one of the non-bridging oxygens of the γ-phosphate of ATP as seen in the structure of the complex with Ap_5T, thereby contributing to the exact positioning of all the reactants and stabilizing the transition state. This is inferred from the superimposed structures of the complex of Ap_5T with the enzymes from *E. coli* (19) and/or *H. sapiens* (17) with the *M. tuberculosis* TMPK-TMP structure (15).

In the human enzyme, a magnesium ion is found on the ATP molecule. Since *M. tuberculosis* TMP kinase has been crystal-

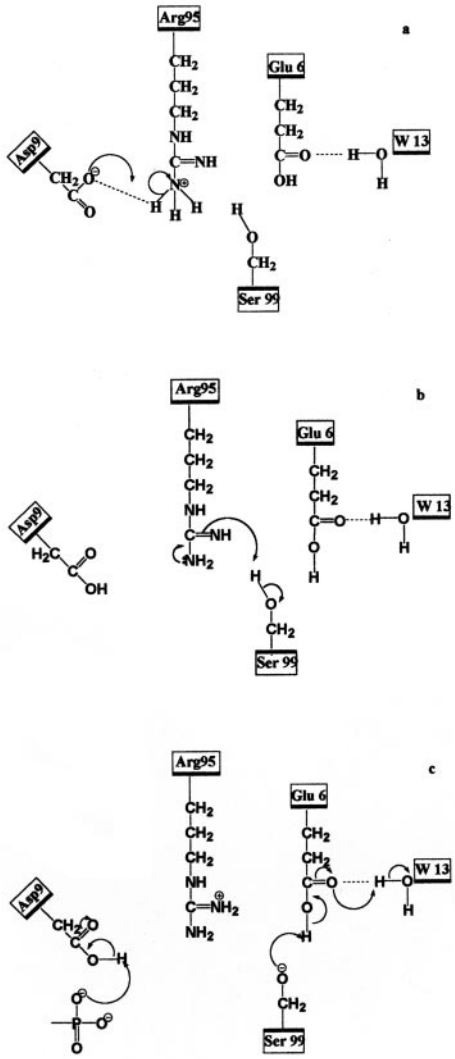

FIG. 6. **Proton wire involving Glu^6, Ser^{99}, Arg^{95}, and Asp^9.** Glu^6 and Ser^{99} are the only non-glycine residues strictly conserved among all known TMPK sequences, Arg^{95} has only one exception (where it is replaced by an histidine), and Asp^9 is always either an aspartate or a glutamate residue (15). *a*, Asp^9 gets its proton from Arg^{95}. *b*, Arg^{95} gets its proton back from Ser^{99}. *c*, Ser^{99} draws a proton from water through Glu^6, while Asp^9 gives its proton to the newly transferred phosphoryl group.

lized only in the presence of TMP, one can only speculate about the presence of a second magnesium ion in the active site when ATP is bound. This (ATP-bound) second magnesium ion, weakening the bond between the β- and γ-phosphates and therefore assisting in the departure of the leaving group, is a general feature of various kinases and is therefore expected also in the *M. tuberculosis* enzyme (43). Two magnesium ions in the active site of kinases would not be surprising as this has been observed in several instances already. However, looking again at the multialignment of all known TMP kinases sequences (15), one notices that Thr^{14} of the Walker A motif, which is essential in the coordination of this second magnesium ion, is not conserved in both *M. leprae* and *M. tuberculosis* sequences. Instead it is replaced by an arginine residue whose guanidinium group can easily be brought, through a simple χ-1 rotation, to the expected binding site of the ATP-bound Mg^{2+} ion.

The next surprising point is that most crystal soaking experiments did not work, indicating that the TMP molecule could not be exchanged at least in the conformation of the enzyme that has been captured in the crystal. In very much the same way, most co-crystallizations did not work (except for **1**), indicating the inability of the analogues tried here to induce the conformational change leading to the form of the enzyme that crystallizes, namely the closed form. Our current interpretation is that the crystal structure has trapped an intermediate already well engaged along the reaction coordinate pathway: most of the inhibitors described here exert their binding abilities on a more open form of the enzyme but are unable to induce the transition from this open form to the closed form. In that sense, the transition to the closed form deserves the name of an induced fit mechanism (44, 45). *M. tuberculosis* TMP kinase is unique among the other known crystal structures of TMP kinases in that the closed form is already formed upon TMP binding with the ATP binding site clearly preformed, whereas virtually all other NMP kinases need the binding of the two substrates to be in the fully closed form (16–20). Two extrinsic factors contribute to this phenomenon: one is the Mg^{2+} ion, and the other is the sulfate ion, which drives the closing and the disorder-order transition of the LID region and which comes from the precipitating agent used to obtain crystals. The Mg^{2+} role has been mentioned above while discussing the inhibition by AZTMP. The role of the sulfate is worth discussing in light of the Ap_5T complex structure.

Although the ATP binding site is preformed in our crystal form, the "ADP" part of Ap_5T was found to bind to an unexpected site. This probably results from the inability of Ap_5T to displace the strongly bound sulfate ion that is located at the ATP β-phosphate binding site. Since this sulfate ion comes from the mother liquor of crystallization, the alternative binding mode of the ADP moiety of Ap_5T might be seen as an artifact of crystallization. However, since it already binds well into a cavity on the surface of the molecule for which it has not been especially designed, it is easy to imagine how one might improve its binding energy. For instance, it might be possible to take advantage of the close proximity of Glu^{55} to C-2 of the adenine ring and of Glu^{50} and Asp^{46} to two different water molecules bound to the 2′- and 3′-position of ADP. It should then be possible to design new drugs against TMP kinase by synthesizing branched molecules at the α-phosphate of Ap_5T with an extra chemical group reaching out to this cavity that is present only in the *M. tuberculosis* enzyme and designed specifically to bind there.

An important finding of the present study is the structural characterization of the binding of TMPK to compound **1**. The structure partly verifies our expectation, by showing an anticipated hydrogen bond between **1** and a known water molecule (W12 in Protein Data Bank structure 1G3U), and partly brings a surprise, by displaying an alternative binding mode with the hydroxyl group pointing toward the network of interactions between Glu^6, Arg^{95}, Tyr^{179}, and Ser^{99}. Both binding modes contribute to the rigidification of the TMP binding pocket and explain why this compound is an inhibitor rather than a substrate, compared with 5-I-dUMP (13, 15), of comparable volume.

We now discuss in more detail the role of Ser^{99}, a strictly conserved residue whose function has remained unclear up to now. First, we observe that the network of interactions in which Ser^{99} is involved contains Glu^6, the only other *non-glycine strictly conserved residue* among all known TMPK sequences (15), as well as Arg^{95}, which is almost universally conserved (except for one exception of 32 sequences where it is an histidine). It is tempting therefore to assume a central role in catalysis for this cluster of interacting residues.

In fact, we can describe this structural catalytic core as a "proton wire" in the active site of TMP kinases, *i.e.* a continuous chain of several side chains in line and sharing a proton including W13, Glu^6, Ser^{99}, Arg^{95}, and Asp^9 (Fig. 6). W13 is in contact with the solvent, so this proton wire couples Asp^9 to a reservoir of water molecules (and protons). Asp^9, which is al-

ways either an aspartate or a glutamate in all known TMPK sequences, is within hydrogen bond distance of two non-bridging oxygens of phosphates, one from the α-phosphate of TMP (acceptor) and the other from the γ-phosphate of ATP (donor). The distances between the residues in this proton wire are within 2.55–2.85 Å with the exception of one definitely weak link between Arg^{95} and Asp^{9} (3.19 Å). We suggest that this distance becomes shorter upon ATP binding, making it possible to consider the Ser^{99}-Arg^{95}-Asp^{9} set as yet another variation of the well known catalytic triad of serine proteases (Ser-His-Asp/Glu). Asp^{9} could get a proton from Arg^{95} (Fig. 6*a*), which immediately gets reprotonated from Ser^{99} and Glu^{6} (Fig. 6, *b* and *c*). The role of Asp^{9} would then be to provide the proton for the transferred phosphoryl group, playing the role of a general acid (Fig. 6*c*). We believe that the proton from the hydroxyl group of the 5′-phosphate of TMP has already been removed by the Mg^{2+} ion. In that sense, we are one step further along the reaction pathway compared with all other transition-state analogue complex structures of other TMPKs. To sustain this hypothesis, we note that catalytic triads show considerable variation of sequence in the three different positions of the classical catalytic triad (46). There is even one case where the histidine residue is replaced by a lysine, so arginine is not inconceivable between a serine and an aspartate (46). Second, it has recently been observed that a previously hitherto unidentified catalytic triad is present in different families of cellulases where the Asp/Glu residue plays the role of a proton donor (47). Third, the recent work of Hutter and Helms (48) urges one to find a proton donor since their quantum molecular mechanics calculations point to a concerted phosphoryl transfer mechanism involving the synchronous shift of a proton from the nucleotide monophosphate to the transferred PO_3 in the related enzyme UMP/CMP kinase. According to these authors (48), most of the activation energy of the phosphoryl transfer is spent on moving the proton toward its destination on the γ-phosphate group, so it is perhaps not surprising to find that TMP kinases have evolved such a sophisticated network of four interacting highly conserved residues to accomplish this process.

Acknowledgments—We thank D. Bourgeois for useful discussions concerning the catalytic mechanism. We thank O. Bârzu for carefully reading the manuscript. V. Vanheusden is indebted to the Fonds voor Wetenschappelijk Onderzoek-Flaanderen for a position of Aspirant.

REFERENCES

1. Stokstad, E. (2000) *Science* **287,** 2391
2. Cole, S. T. (1994) *Trends Microbiol.* **2,** 411–415
3. Tsuyuguchi, I. (2001) *Tuberculosis* **81,** 221–227
4. Anderson, E. P. (1973) in *The Enzymes* (Boyer, P. D., ed) 3rd Ed., Vol. 8, pp. 49–96, Academic Press, New York
5. Dabry, G. K. (1995) *Antiviral Chem. Chemother.* **6,** 54–63
6. Griffiths, P. D. (1995) *Antiviral Chem. Chemother.* **6,** 191–209
7. Champness, J. N., Bennett, M. S., Wien, F., Visse, R., Summers, W. C., Herdewijn, P., De Clercq, E., Ostrowski, T., Jarvest, R. L., and Sanderson, M. R. (1998) *Proteins Struct. Funct. Genet.* **32,** 350–361
8. Bennett, M. S., Wien, F., Champness, J. N., Batuwangala, T., Rutherford, T., Summers, W. C., Sun, H., Wright, G., and Sanderson, M. R. (1999) *FEBS Lett.* **443,** 121–125
9. Wild, K., Bohner, T., Folkers, G., and Schlulz, G. E. (1997) *Protein Sci.* **6,** 2097–2106
10. Vogt, J., Perozzo, R., Pautsch, A., Prota, A., Schelling, P., Pilger, B., Folkers, G., Scapozza, L., and Schulz, G. E. (2000) *Proteins* **41,** 545–551
11. Manallack, D., Pitt, W. R., Herdewijn, P., Balzarini, J., De Clercq, E., Sanderson, M. R., Sohi, M., Wien, F., Munier-Lehmann, H., Haouz, A., and Delarue, M. (2002) *J. Enzyme Inhib. Med. Chem.* **17,** 167–174
12. de Winter, H., and Herdewijn, P. (1996) *J. Med. Chem.* **39,** 4727–4737
13. Munier-Lehmann, H., Chaffotte, A., Pochet, S., and Labesse, G. (2001) *Protein Sci.* **10,** 1195–1205
14. Li de la Sierra, I., Munier-Lehmann, H., Gilles, A. M., Bârzu, O., and Delarue, M. (2000) *Acta Crystallogr. Sect. D Biol. Crystallogr.* **56**, 226–228
15. Li de la Sierra, I., Munier-Lehmann, H., Gilles, A. M., Bârzu, O., and Delarue, M. (2001) *J. Mol. Biol.* **311,** 87–100
16. Ostermann, N., Lavie, A., Padiyar, S., Brundiers, R., Veit, T., Reinstein, J., Goody, R. S., Konrad, M., and Schlichting, I. (2000) *J. Mol. Biol.* **304,** 43–53
17. Ostermann, N., Schlichting, I., Brundiers, R., Konrad, M., Reinstein, J., Goody, R. S., and Lavie, A. (2000) *Structure* **8,** 629–642
18. Lavie, A., Konrad, M., Brundiers, R., Goody, R. S., Schlichting, I., and Reinstein, J. (1998) *Biochemistry* **37,** 3677–3686
19. Lavie, A., Ostermann, N., Brundiers, R., Goody, R., Reinstein, J., Konrad, M., and Schlichting, I. (1998) *Proc. Natl. Acad. Sci. U. S. A.* **95,** 14045–14050
20. Lavie, A., Vetter, I., Konrad, M., Goody, R. S., Reinstein, J., and Schlichting, I. (1997) *Nat. Struct. Biol.* **4,** 601–605
21. Vanheusden, V., Munier-Lehmann, H., Pochet, S., Herdewijn, P., and Van Calenbergh, S. (2002) *Bioorg. Med. Chem. Lett.* **12,** 2695–2698
22. Kleywegt, G., and Jones, T. A. (1994) *Acta Crystallogr. Sect. D Biol. Crystallogr.* **50**, 178–185
23. Ostrowski, T., Wroblowski, R., Busson, R., Rozenski, J., De Clercq, E., Bennett, M. S., Champness, J. N., Summers, W. C., Sanderson, M. R., and Herdewijn, P. (1998) *J. Med. Chem.* **41,** 4343–4353
24. Vastmans, K., Froeyen, M., Kerremans, L., Pochet, S., and Herdewijn, P. (2001) *Nucleic Acids Res.* **29,** 3154–3163
25. Cline, R. E., Fink, R. M., and Fink, K. (1958) *J. Am. Chem. Soc.* **80,** 2521–2525
26. Scheit, K. H. (1966) *Chem. Ber.* **99,** 3884–3891
27. Tona, R., Bertolini, R., and Hunziker, J. (2000) *Org. Lett.* **2,** 1693–1696
28. Gupta, V. S., and Bubbar, G. L. (1971) *Can. J. Chem.* **49,** 719–722
29. Wigerinck, P., Pannecouque, C., Snoeck, R., Claes, P., De Clercq, E., and Herdewijn, P. (1991) *J. Med. Chem.* **34,** 2383–2389
30. Blondin, C., Serina, L., Wiesmuller, L., Gilles, A. M., and Bârzu, O. (1994) *Anal. Biochem.* **220,** 219–221
31. Haouz, A., Geleso-Meyer, A., and Burstein, C. (1994) *Enzyme Microb. Technol.* **16,** 292–297
32. Otwinowski, Z., and Minor, W. (1997) *Methods Enzymol.* **276,** 307–326
33. CCP4 (1994) *Acta Crystallogr. Sect. D Biol. Crystallogr.* **50**, 760–763
34. Brunger, A. T., Adams, P. D., Clore, G. M., DeLano, W. L., Gros, P., Grosse-Kunstleve, R. W., Jiang, J. S., Kuszewski, J., Nilges, M., Pannu, N. S., Read, R. J., Rice, L. M., Simonson, T., and Warren, G. L. (1998) *Acta Crystallogr. Sect. D Biol. Crystallogr.* **54**, 905–921
35. Murshudov, G., Vagin, A., and Dodson, E. (1997) *Acta Crystallogr. Sect. D Biol. Crystallogr.* **53**, 240–255
36. Read, R. J. (1986) *Acta Crystallogr. Sect. A* **42,** 140–149
37. Jones, T. A., Zou, J. Y., Cowan, S. W., and Kjeldgaard, M. (1991) *Acta Crystallogr. Sect. A* **47**, 110–119
38. Laskowski, R. A., McArthur, M. W., Moss, D. S., and Thornton, J. M. (1993) *J. Appl. Crystallogr.* **21,** 283–291
39. Segel, I. H. (1993) *Enzyme Kinetics*, Wiley-Interscience Publications, John Wiley, New York
40. Jencks, W. P. (1987) *Catalysis in Chemistry and Enzymology*, Dover Publications, New York.
41. Scheffzek, K., Kliche, W., Wiesmüller, L., and Reinstein, J. (1996) *Biochemistry* **35,** 9716–9727
42. Sheng, X. R., Li, X., and Pan, X. M. (1999) *J. Biol. Chem.* **274,** 22238–22242
43. Cheek, S., Zhang, H., and Grishin, N. V. (2002) *J. Mol. Biol.* **320,** 855–881
44. Schulz, G. E., Muller, C. W., and Diederichs, K. (1990) *J. Mol. Biol.* **213,** 627–630
45. Muller, C. W., Schlauderer, G. J., Reinstein, J., and Schulz, G. E. (1996) *Structure* **4,** 147–156
46. Dodson, G., and Wlodawer, A. (1998) *Trends Biochem. Sci.* **23,** 347–352
47. Shaw, A., Bott, R., Vonrhein, C., Bricogne, G., Power, S., and Day, A. G. (2002) *J. Mol. Biol.* **320,** 303–309
48. Hutter, M. C., and Helms, V. (2000) *Protein Sci.* **9,** 2225–2231
49. Esnouf, R. (1999) *Acta Crystallogr. Sect. D Biol. Crystallogr.* **55**, 938–940
50. Nicholls, A., Sharp, K., and Honig, B. (1991) *Proteins* **11,** 281–291